Comunicaciones Nº 43 (1992): 57 - 71

EVOLUTION AND ZONING OF AU/AG MINERALIZATION IN THE CAN CAN EPITHERMAL SYSTEM, MARICUNGA BELT: FLUID INCLUSION EVIDENCE

EVOLUCION Y ZONACION DE LA MINERALIZACION DE AU/AG EN EL SISTEMA EPITERMAL CAN CAN, FRANJA MARICUNGA: EVIDENCIA DE INCLUSIONES FLUIDAS

Brian K. Townley

Departamento de Geología, Universidad de Chile
Casilla 13518, correo 21, Stgo., Chile

RESUMEN

El depósito Can Can, ubicado 140 km al NE de Copiapó, puede ser clasificado como un sistema epitermal de Au/Ag del tipo sulfidización alta. La roca de caja corresponde a lutitas, areniscas y conglomerados de la formación La Ternera (Triásico) y a tobas dacíticas del complejo volcánico Maricunga-Vicuñita (Oligoceno). Este depósito muestra un fuerte control estructural de orientación principal NE-SW y está genéticamente relacionado a la intensa actividad volcánica terciaria. La alteración predominante está caracterizada por silicificación intensa y alteración cuarzo-alunita, con grados menores de alteración argílica y propilítica. La mineralización de mena consiste en Au, Ag y cantidades menores de Cu. El Au y Ag están presentes en forma nativa, pero la Ag es más frecuente como cerargirita. La razón Au/Ag es más alta en niveles más bajos del sistema y decrece rápidamente con el ascenso en cota hacia la superficie.

Los estudios de inclusiones fluidas indican temperaturas de homogeneización (Th) entre 170 y 350° C, donde se presenta una diferenciación de dos grupos principales de inclusiones fluidas de dos fases (tipo A y B), caracterizados por el porcentaje de la fase de vapor, su forma y disposición espacial. Las inclusiones de tipo A muestran un Th entre 170 y 290° C con un valor promedio de 223° C, mientras que los de tipo B muestran un Th entre 190 y 350° C con un valor promedio de 258° C. Los valores de salinidad indican un aporte en profundidad de soluciones de alta salinidad, con un marcado descenso de salinidad con el ascenso a través del sistema, con valores que van desde 40 hasta 1% NaCl equivalente (eq) o más bajo. Las inclusiones de tipo A muestran una salinidad promedio de 11.1% NaCl eq. mientras que las de tipo B muestran un valor promedio de 9.45% NaCl eq. La distribución de salinidad versus Th sugiere en ambos casos la posibilidad de ebullición. Observación directa de las inclusiones fluidas indica la presencia de zonas de ebullición, uno a una cota

---

Contribución Nº 996

de 4050 msnm, con un valor de Th promedio de 234° C y salinidad promedio de 16.6% NaCl % eq., y otro a una cota de 3950 msnm, con un Th promedio de 275° C y salinidad y promedio de 10.3% NaCl eq. La profundidad calculada para las zonas de ebullición indican preservación de la paleosuperficie, lo cual está de acuerdo con las observaciones de terreno.

La existencia de dos familias de inclusiones fluidas puede ser asociado a las dos zonas de ebullición. Esto podría estar representando dos etapas de actividad hidrotermal durante la evolución del sistema, lo cual es consistente con la zonación de Au y Ag. La mineralización de Ag puede ser asociada a una etapa, más alta en cota, más baja en temperatura y de mayor salinidad. La mineralización de Au queda entonces asociada a una segunda etapa, más baja en cota y de menor extensión areal, dando lugar a depositación de Au-Ag por debajo del extenso horizonte de Ag. De esta forma, la evolución de este sistema epitermal permite explicar la zonación de Au y Ag en Can Can.

SUMMARY

Can Can, located 140 km NE of Copiapó, can be classified as an acid sulfate Au/Ag epithermal deposit. It is hosted by shales, sandstones and conglomerates of the La Tenera formation (Triassic) and dacitic tuffs of the Maricunga-Vicuñita complex (Oligocene). This deposit shows strong structural control by NE-SW striking faults and is genetically related to intense Tertiary volcanism. Alteration is characterized by intense silification and quartz-alunite, with less intensive argillic and propylitic alteration. Ore mineralization consists of Au, Ag and minor Cu. Au and Ag are present in native form, but Ag appears more commonly as cerargyrite. Au/Ag ratios are higher in lower levels of the system, decreasing rapidly up towards surface levels.

Fluid inclusion studies indicate homogenization temperatures (Th) between 170 and 350° C, with distintion of two main groups of two phase fluid inclusions (type A and B), characterized by vapor phase percentage, form and disposition. Type A fluid inclusions have a Th between 170 and 290° C with a mean value of 223° C, while type B have a Th between 190 and 350° C with a mean value of 258° C. Salinity values indicate strong influx of higher saline fluids at depth with decreasing salinities towards higher elevations in the system, showing values ranging from 40 to 1% NaCl equivalent (eq.) or lower. Type A fluid inclusions have a mean salinity value of 11.1% NaCl eq., while type B have a mean value of 9.5% NaCl eq. Th vs. salinity distribution suggest boiling in both cases, while direct observation of fluid inclusions indicates existence of two boiling zones, one at an elevation of 4050 m., with a mean Th value of 234° C and salinity value of 16.6% NaCl eq., and another at an elevation of 3950 m., with a mean Th value of 275° C and salinity value of 10.3% NaCl eq. Depth calculated for boiling zones according to fluid inclusion data indicate preservation of the paleosurface, which is in accordance with field observations.

Existence of two families of fluid inclusions can be associated with the two boiling zones. These could represent two stages of hydrothermal activity during the evolution of the system, which is consistent with Au/Ag mineral zoning. Extensive Ag mineralization can be associated with one stage, higher in elevation, lower in temperature and higher in salinity. Au mineralization is then associated with a second stage of hydrothermal activity, lower in elevation and less extensive, depositing Au-Ag below the extensive Ag horizon. Evolution of this epithermal system allows an explanation for Au/Ag zoning in Can Can.

INTRODUCTION

Can Can is located in the III Region of Chile, aproximately 140 km. northwest of Copiapó (Fig. 1), 26°48' south latitude and 69°16' west longitude, with a mean elevation of 4200 m. The main access road is the international road CH-31, between the cities of Copiapó and Tinogasta (Argentina).

The Can Can epithermal Au/Ag deposit is one of numerous precious metal epithermal systems discovered in the Maricunga Au/Ag epithermal belt. This epithermal system can be classified as acid sulfate type, where silification and intense quartz-alunite alteration predominate. Explored by Sierra Morena S. A. and Chevron Minera Corporation of Chile, abundant information on alteration and mineralization is available, which, interpreted and compared with fluid inclusion studies will give a global vision of this epithermal system.

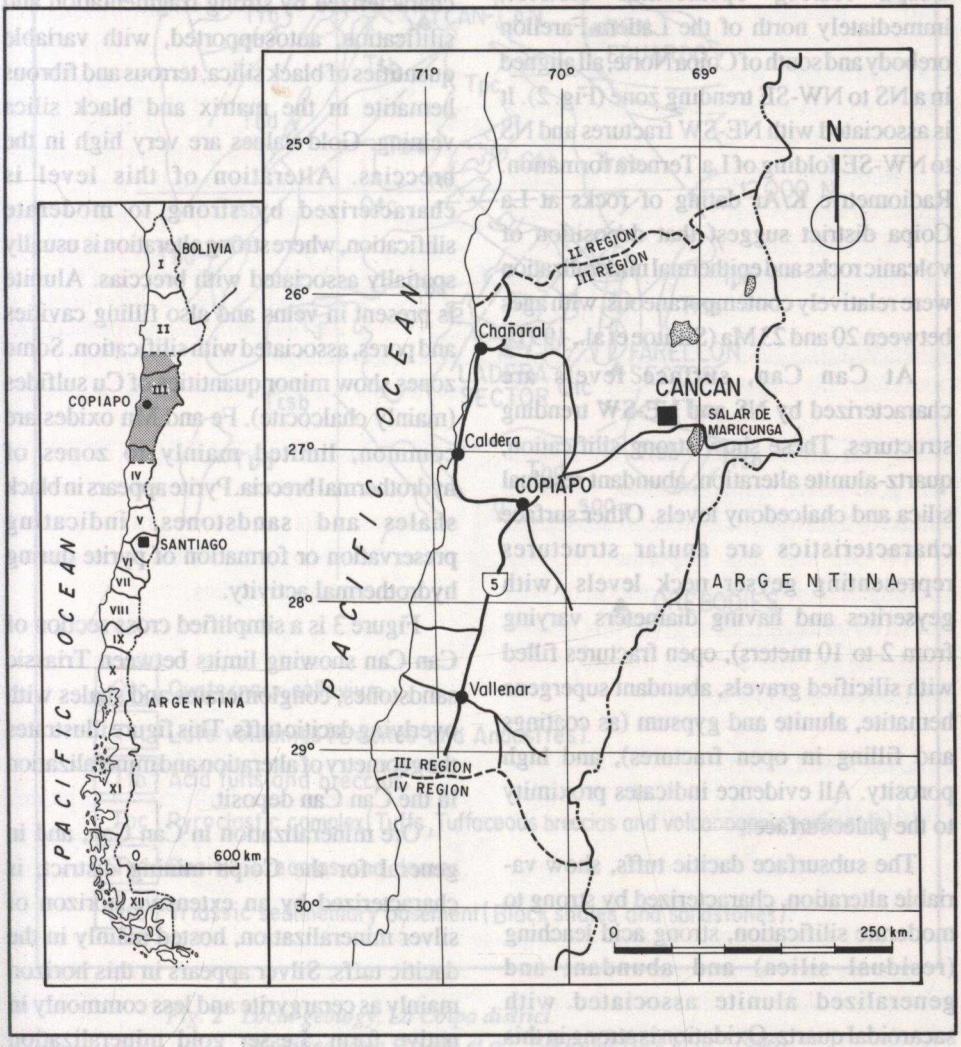

Fig. 1 Location map.
Plano de ubicación.

GEOLOGICAL SETTING

The Can Can epithermal system is hosted by black shales, conglomerates and sandstones of the La Ternera Formation, of upper Triassic and lower Jurassic age (Brüggen, 1917; 1950), and dacitic to ryodacitic tuffs belonging to the Maricunga-Vicuñita volcanic complex, of the upper Oligocene and Miocene age (Aguilar, 1984). It is one of the orebodies belonging to the Coipa Au/Ag epithermal district, immediately north of the Ladera-Farellón orebody and south of Coipa Norte, all aligned in a NS to NW-SE trending zone (Fig. 2). It is associated with NE-SW fractures and NS to NW-SE folding of La Ternera formation. Radiometric K/Ar dating of rocks at La Coipa district suggest that deposition of volcanic rocks and epithermal mineralization were relatively contemporaneous, with ages between 20 and 23 Ma (Sillitoe et al., 1991).

At Can Can, surface levels are characterized by NS and NE-SW trending structures. These show strong silification, quartz-alunite alteration, abundant residual silica and chalcedony levels. Other surface characteristics are anular structures representing geyser neck levels (with geyserites and having diameters varying from 2 to 10 meters), open fractures filled with silicified gravels, abundant supergene hematite, alunite and gypsum (as coatings and filling in open fractures), and high porosity. All evidence indicates proximity to the paleosurface.

The subsurface dacitic tuffs, show variable alteration, characterized by strong to moderate silification, strong acid leaching (residual silica) and abundant and generalized alunite associated with sacaroidal quartz. Oxidation is strong in this level, characterized by abundant jarosite, hematite and limonite, together with lesser quantities of Mn oxides. Various hydrothermal breccias exist at this level, characterized mainly by strong oxidation and silification.

The lower levels of the system are hosted by black shales, sandstones and conglomerates which show some sedimentary structures such as cross stratification, impact folds and ripple marks. Hydrothermal breccias are less common and more constricted than in higher levels, characterized by strong fragmentation and silification, autosupported, with variable quantities of black silica, terrous and fibrous hematite in the matrix and black silica veining. Gold values are very high in the breccias. Alteration of this level is characterized by strong to moderate silification, where strong alteration is usually spatially associated with breccias. Alunite is present in veins and also filling cavities and pores, associated with silification. Some zones show minor quantities of Cu sulfides (mainly chalcocite). Fe and Mn oxides are common, limited mainly to zones of hydrothermal breccia. Pyrite appears in black shales and sandstones, indicating preservation or formation of pyrite during hydrothermal activity.

Figure 3 is a simplified cross section of Can Can showing limits between Triassic sandstones, conglomerates and shales with overlying dacitic tuffs. This figure illustrates the geometry of alteration and mineralization in the Can Can deposit.

Ore mineralization in Can Can, and in general for the Coipa mining district, is characterized by an extensive horizon of silver mineralization, hosted mainly in the dacitic tuffs. Silver appears in this horizon mainly as cerargyrite and less commonly in native form. Lesser gold mineralization appears with silver, and some vein and breccia zones rich in gold are recognized.

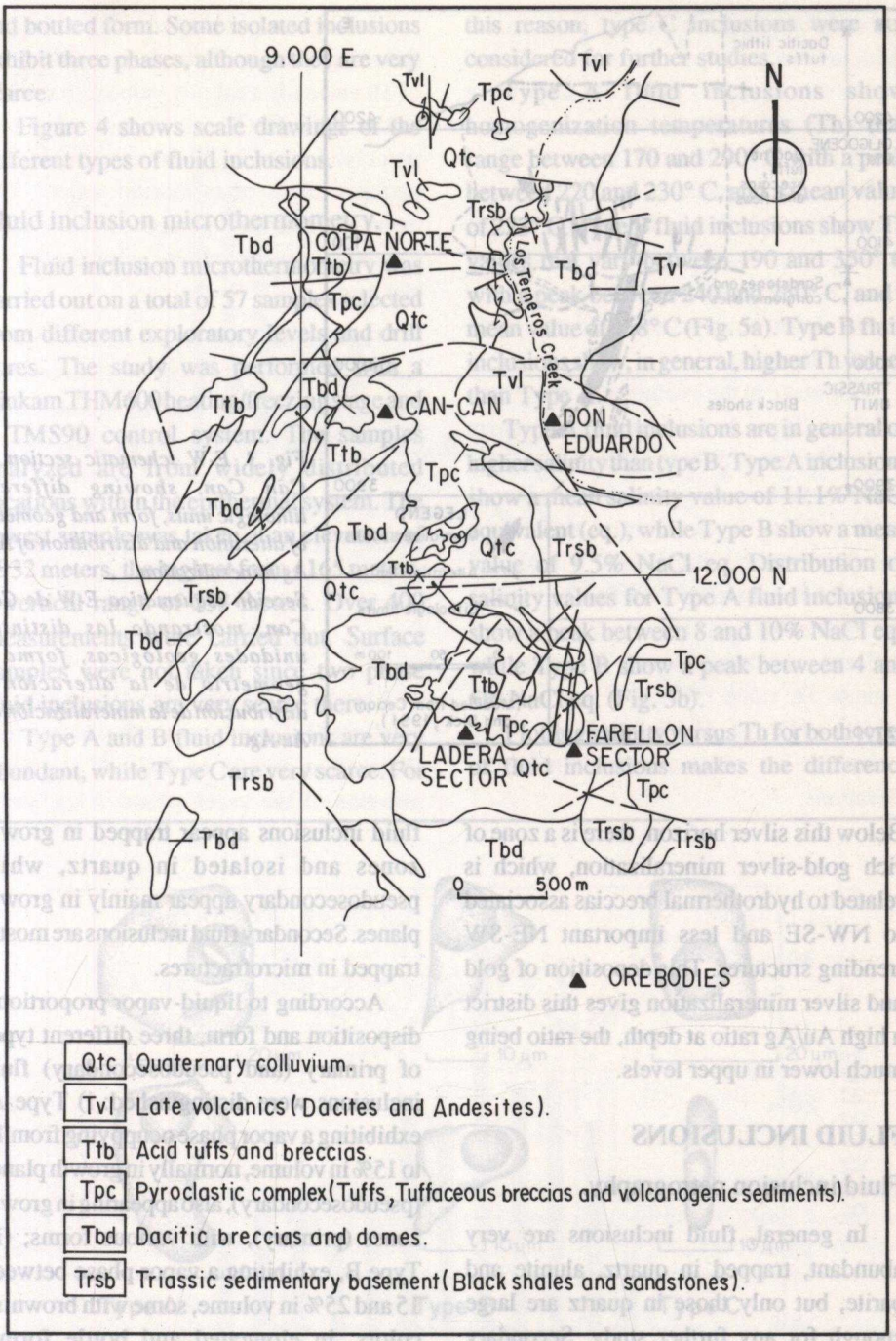

Fig. 2 Local geology, La Coipa district.
(Modified from Oviedo et al., 1991 and Dick et al., 1990).
Geología local, distrito La Coipa.
(Modificado de Oviedo et al., 1991, y Dick et al., 1990).

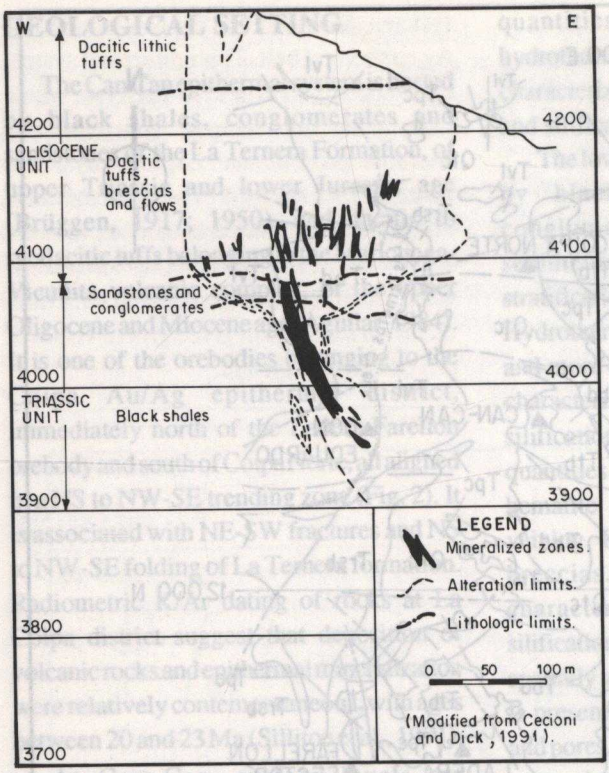

Fig. 3. E-W schematic section of Can Can, showing different lithologic units, form and geometry of alteration and distribution of Au-Ag mineralization.
Sección esquemática E-W de Can Can, mostrando las distintas unidades geológicas, forma y geometría de la alteración y distribución de la mineralización de Au-Ag.

Below this silver horizon, there is a zone of rich gold-silver mineralization, which is related to hydrothermal breccias associated to NW-SE and less important NE-SW trending sructures. This deposition of gold and silver mineralization gives this district a high Au/Ag ratio at depth, the ratio being much lower in upper levels.

FLUID INCLUSIONS

Fluid inclusion petrography.

In general, fluid inclusions are very abundant, trapped in quartz, alunite and barite, but only those in quartz are large enough for any further study. Secondary fluid inclusions dominate over primary, but both are very abundant. Only primary and pseudosecondary fluid inclusions were considered for microthermometry. Primary fluid inclusions appear trapped in growth zones and isolated in quartz, while pseudosecondary appear mainly in growth planes. Secondary fluid inclusions are mostly trapped in microfractures.

According to liquid-vapor proportions, disposition and form, three different types of primary (and pseudosecondary) fluid inclusions were distinguished: i) Type A, exhibiting a vapor phase ocuppying from 10 to 15% in volume, normally in growth planes (pseudosecondary), also appearing in growth zones (primary), with various forms; (ii) Type B, exhibiting a vapor phase between 15 and 25% in volume, some with brownish colors, in elongated and bottle forms, generally perpendicular in growth zones and also in growth planes; iii) Type C, exhibiting a vapor phase between 10 and 20%, appearing only in isolated, elongated,

and bottled form. Some isolated inclusions exhibit three phases, although they are very scarce.

Figure 4 shows scale drawings of the different types of fluid inclusions.

Fluid inclusion microthermometry.

Fluid inclusion microthermometry was carried out on a total of 57 samples selected from different exploratory levels and drill cores. The study was performed with a Linkam THM600 heating/freezing stage and a TMS90 control system. The samples analyzed are from widely distributed locations within the epithermal system. The lowest sample was taken at an elevation of 3932 meters, the highest from 4165 meters, a vertical range of 233 meters. Over 400 measurements were carried out. Surface samples were not taken since two phase fluid inclusions are very scarce there.

Type A and B fluid inclusions are very abundant, while Type C are very scarce. For this reason, type C inclusions were not considered for further studies.

Type A fluid inclusions show homogenization temperatures (Th) that range between 170 and 290° C with a peak between 220 and 230° C, and a mean value of 223° C. Type B fluid inclusions show Th values that vary between 190 and 350° C with a peak between 240 and 250° C, and a mean value of 258° C (Fig. 5a). Type B fluid inclusions show, in general, higher Th values than Type A.

Type A fluid inclusions are in general of higher salinity than type B. Type A inclusions show a mean salinity value of 11.1% NaCl equivalent (eq.), while Type B show a mean value of 9.5% NaCl eq. Distribution of salinity values for Type A fluid inclusions show a peak between 8 and 10% NaCl eq., while Type B show a peak between 4 and 6% NaCl eq. (Fig. 5b).

Plotting salinity versus Th for both types of fluid inclusions makes the difference

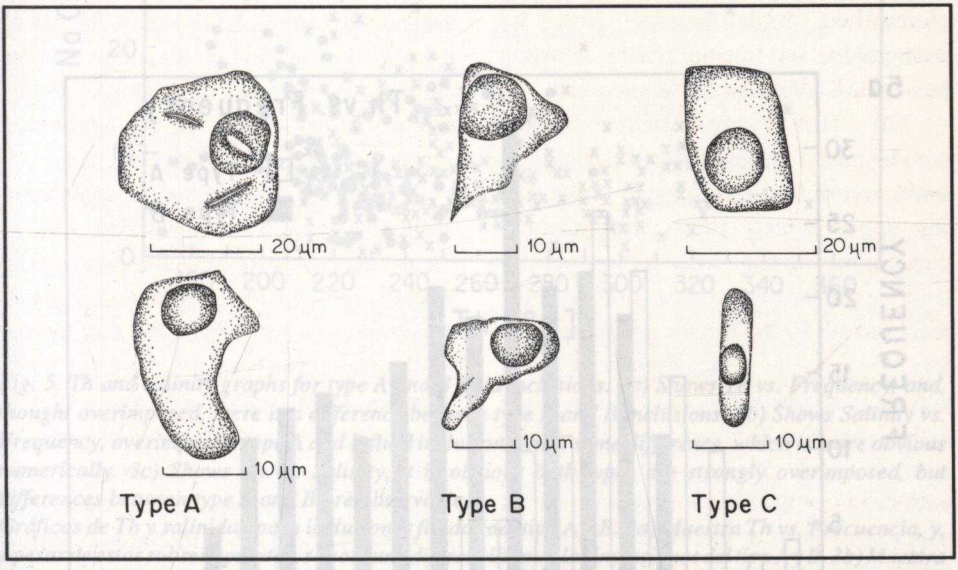

Fig. 4. Schematic drawings of type A, B and C fluid inclusions, differentiated by vapor phase percentage in volume, form and disposition. Type C are very uncommon.
Bosquejos esquemáticos de inclusiones fluidas del tipo A, B y C, diferenciadas por su porcentaje en volumen de la fase vapor, forma y disposición. Los del tipo C son muy poco frecuentes.

between them more obvious (Fig. 5c). Type A inclusions are in general of lower Th and higher salinity than Type B, but show more dispersion of data. These differences suggest the possibility that both types of fluid inclusions were generated in different stages during the evolution of the system. This is confirmed by the fact that mixture of Type A and B fluid inclusions in the same quartz crystal almost never occurs, except for those that are annealed.

One stage in the evolution of the system involves Type A fluid inclusions, where larger dispersion of data and higher salinity of the inclusions suggest a strong influx of high salinity hydrothermal solutions, possibly of magmatic origin. Mixture of these fluids with meteoritic fluids give rise to a wide zone of mixing, which is observed in all ranges of temperatures. This stage has a mean Th value of 223° C and a mean salinity value of 11.1% NaCl eq. These inclusions are most abundant in higher elevations.

A second stage was associated with Type B fluid inclusions. These show a wide range of Th values, but salinity values are usually below 10% NaCl eq., suggesting lower participation of high salinity fluids and stronger influx of meteoritic waters. The mean Th value for this second event is 258° C, while the mean salinity value is of 9.5% NaCl eq.

The abundance of Type B fluid inclusions and the fact that Type A become less common with depth suggests that the second stage represents late hydrothermal activity during the evolution of the system. These two stages probably represent major hydrothermal events, but each stage could be represented by many shorter hydrothermal events.

Boiling Zones

Two boiling zones were determined by petrographic and microthermometric observation criteria as follows: i) strong variation of the vapor phase in the same

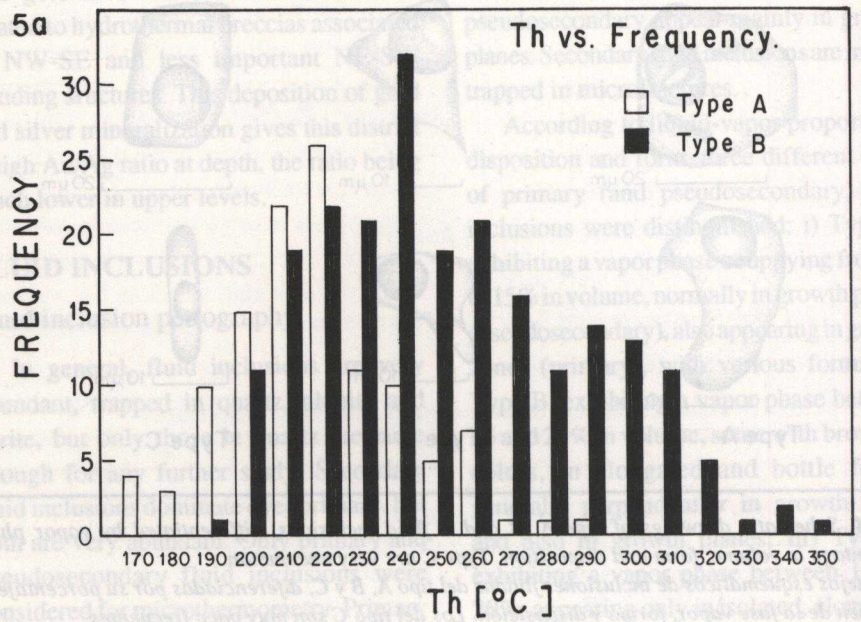

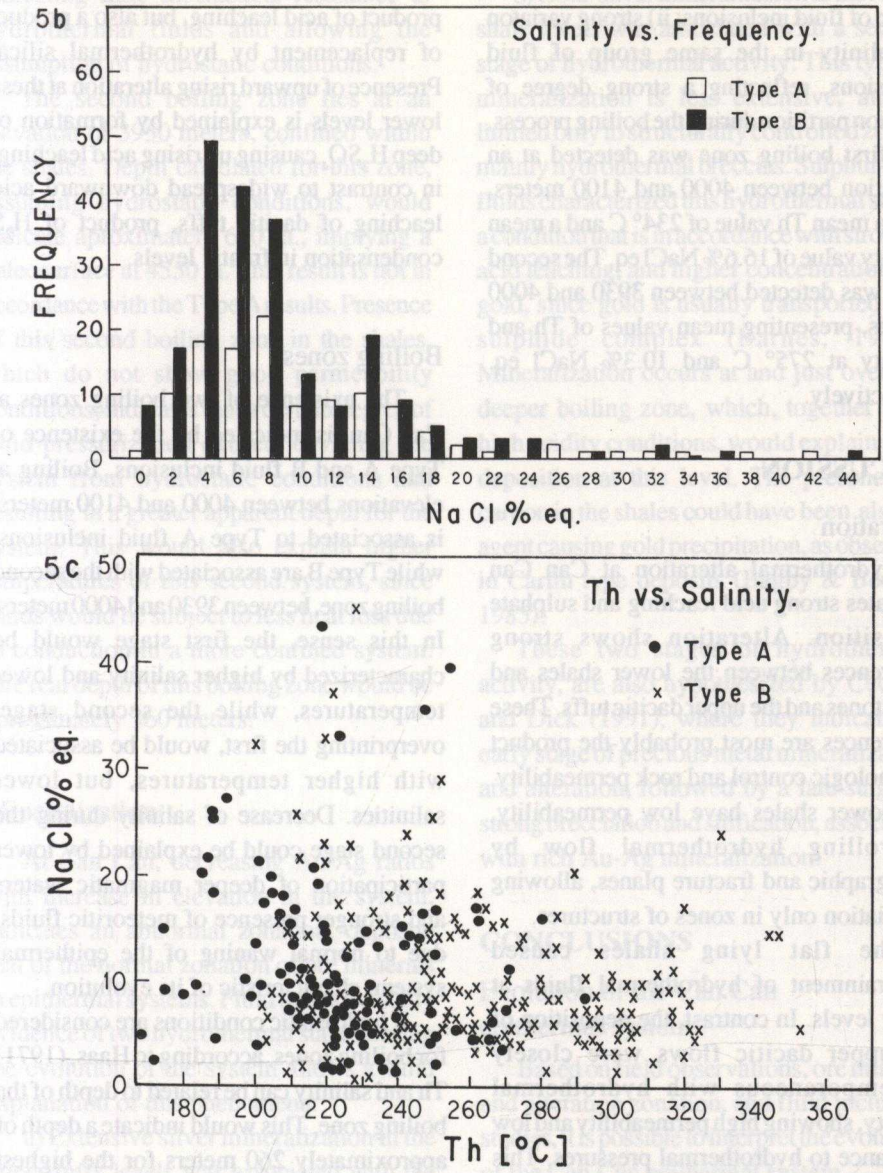

Fig. 5. Th and salinity graphs for type A and B fluid inclusions. 3a) Shows Th vs. Frequency, and, thought overimposed, there is a difference between type A and B inclusions. 3b) Shows Salinity vs. Frequency, overimposed, type A and B fluid inclusions show some difference, which is more obvious numerically. 3c) Shows Th vs. Salinity, it is obvious both types are strongly overimposed, but differences between type A and B are observable.

Gráficos de Th y salinidad para inclusiones fluidas del tipo A y B. 3a) Muestra Th vs. Frecuencia, y, a pesar de estar sobreimpuestos, se nota una diferencia entre las inclusiones del tipo A y B. 3b) Muestra Salinidad vs. Frecuencia, sobreimpuestos, las inclusiones de tipo A y B muestran una pequeña diferencia, la cual es más notable en forma numérica. 3c) Muestra Th vs. Salinidad, haciendo evidente la sobreimposición existente entre las inclusiones de ambos tipos, pero, las diferencias entre ambos son apreciables.

group of fluid inclusions; ii) strong variaton of salinity in the same group of fluid inclusions, reflecting a strong degree of solution partition during the boiling process. The first boiling zone was detected at an elevation between 4000 and 4100 meters, with a mean Th value of 234° C and a mean salinity value of 16.6% NaCl eq. The second zone was detected between 3930 and 4000 meters, presenting mean values of Th and salinity at 275° C and 10.3% NaCl eq. respectively.

DISCUSSION

Alteration

Hydrothermal alteration at Can Can indicates strong acid leaching and sulphate deposition. Alteration shows strong differences between the lower shales and sandstones and the upper dacitic tuffs. These differences are most probably the product of lithologic control and rock permeability. The lower shales have low permeability, controlling hydrothermal flow by stratigraphic and fracture planes, allowing brecciation only in zones of structures.

The flat lying shales caused constrainment of hydrothermal fluids at lower levels. In contrast, the deposition of the upper dacitic flows were closely contemporaneous with hydrothermal activity, showing high permeability and low resistance to hydrothermal pressures. This level gives rise to a funnel shape alteration zone with abundant brecciation. Alteration at this level is widespread and acid leaching is very intense. These processes, together with strong oxidation, give evidence for the water table level at the time of alteration, where mixing of gaseous H_2S with freatic waters resulted in condensation and formation of H_2SO_4. In contrast, silification of the lower shale levels, is not only a product of acid leaching, but also a product of replacement by hydrothermal silica. Presence of upward rising alteration at these lower levels is explained by formation of deep H_2SO_4 causing up rising acid leaching, in contrast to widespread downward acid leaching of dacitic tuffs, product of H_2S condensation in freatic levels.

Boiling zones

The existence of two boiling zones at Can Can, is indicated by the existence of Type A and B fluid inclusions. Boiling at elevations between 4000 and 4100 meters, is associated to Type A fluid inclusions, while Type B are associated with the second boiling zone, between 3930 and 4000 meters. In this sense, the first stage would be characterized by higher salinity and lower temperatures, while the second stage, overprinting the first, would be associated with higher temperatures, but lower salinities. Decrease of salinity during the second stage could be explained by lower participation of deeper magmatic waters and stronger presence of meteoritic fluids, due to normal waning of the epithermal system, characteristic of its evolution.

If hydrostatic conditions are considered for boiling zones, according to Haas, (1971) Th and salinity can be related to depth of the boiling zone. This would indicate a depth of approximately 260 meters for the highest boiling zone, at 4050 meters. It would imply a paleosurface at 4310 meters, which is close to the actual elevation of surface, indicating preservation of the paleosurface. Field observations of surface structures, such as geyserites and open fractures filled by silicified gravels support these results. This boiling zone is practically at the shale-dacite disconformity, where dacitic tuffs show strong brecciation and good permeability,

indicating little mechanical resistance to hydrothermal fluids and allowing the assumption of hydrostatic conditions.

The second boiling zone lies at an elevation of 3950 meters, confined within the shales. Depth calculated for this zone, assuming hydrostatic conditions, would indicate aproximately 600 m., implying a paleosurface at 4550 m. This result is not in accordance with the Type A results. Presence of this second boiling zone in the shales, which do not show good permeability conditions, indicates that a certain degree of fluid pressurization existed, deviating the system from hydrostatic conditions and resulting in a greater apparent depth for the system. This would also explain higher temperatures of this second system, since fluids would be subject to less heat loss due to conduction in a more confined system. The real depth of this boiling zone would be aproximately 360 meters.

Mineralization

At Can Can, decreasing Au/Ag ratios with increase in elevation in the system, indicates an abnormal zonation, opposite that of the normal zonation of ore minerals in epithermal systems. Fluid inclusion study evidence of two hydrothermal stages during the evolution of the system allows a valid explanation of this phenomena:

a) Extensive silver mineralization in the upper tuffs levels was associated with the first stage, which shows a boiling level at the shale-tuff interface. High salinity fluids with temperature ranging from 170 to 290° C represent this hydrothermal stage. Abundance of silver would be in accordance with higher salinity, since silver is transported mainly as a chloride complex, favored by higher salinity concentrations (Barnes, 1967).

b) Gold-silver mineralization in the lower shale levels was associated with a second stage of hydrothermal activity. This type of mineralization is less extensive, and is limited only to structurally controlled zones, mainly hydrothermal breccias. Sulphur-rich fluids characterized this hydrothermal stage, a condition that is in accordance with stronger acid leaching, and higher concentrations of gold, since gold is usually transported as a sulphide complex (Barnes, 1967). Mineralization occurs at and just over the deeper boiling zone, which, together with high acidity conditions, would explain gold deposition at this level. The presence of carbon in the shales could have been also an agent causing gold precipitation, as observed in Carlin type deposits (Bagby & Berger, 1985).

These two stages of hydrothermal activity, are also hypothesized by Cecioni and Dick (1991), where they indicate an early stage of precious metal mineralization and alteration, followed by a late stage of strong brecciation and silification, associated with rich Au-Ag mineralization.

CONCLUSIONS

Evolution of the Can Can epithermal system.

Based on field observations, ore mineral and alteration zonation, and fluid inclusion studies, it is possible to interpret the evolution of the Can Can epithermal system.

Initial stages of hydrothermal activity were directly associated with Tertiary (Miocene) volcanism and strongly controlled by structural systems. The first stage of epithermal activity had a boiling zone aproximately at 4050 meters, probably contemporaneous with deposition of pyroclastic volcanic rocks and intrusion of dacitic domes. This stage was responsible

for deposition of extensive silver mineralization. Strong brecciation and acid leaching of volcanic rocks associated with quartz-alunite alteration and silification occured during the early hydrothermal event. Fluids during this first stage had temperatures wich ranged between 170 and 290° C, with high salinity values, suggesting strong influence of magmatic fluids. Due to brittleness and good permeability of the host rock, the boiling zone of this system would have been practically under hydrostatic conditions, at a depth of aproximately 260 meters.

A second stage of activity, deeper, and constrained within lower shale levels, overprinted the first stage. This stage, with strong overpressurization due to confinement of the boiling zone in low permeability rocks, exhibits a rise in temperature, that ranges between 190 and 350° C. This second stage of activity, lower in salinity and highly acidic, was associated with Au/Ag deposition and strong acid leaching together with very strong brecciation, silification and quartz-alunite alteration. Depth of the boiling zone is estimated at aproximately 360 meters.

Field observations and fluid inclusion evidence indicate preservation of the paleosurface, at 4300 to 4350 meters.

Evolution of the system is schematically presented in figure 6.

Zonation of Au/Ag mineralization in Can Can.

Evolution of the system, according to the previous interpretation, would be in accordance with decreasing Au/Ag ratios with higher elevations in the system. In this sence, anomalous Au and Ag zonation present in Can Can can be explained by existance of two stages of hydrothermal mineralization during evolution of the system. The first, extensive, associated with high silver values in the upper zones of the system, followed by a second stage, more confined, associated with Au and Ag mineralization. This situation (represented schematically in figure 7) is present in other deposits in the Maricunga Belt, such as La Coipa (Oviedo et al., 1991) and Esperanza (Vila, 1991), and could possibly be representing a regional evolution trend, associated with Tertiary volcanic activity.

The coincidence between the evolution of the system, field observations, fluid inclusion studies, alteration zonation, and ore mineralization, give a valid explanation for ore mineral zonation, but it does not discard the possibility of other events or variables controlling ore mineral zonation.

ACKNOWLEDGEMENTS

This work would of been impossible without the generous and constant cooperation and financing given by Chevron Minera Corporation of Chile, through Dr. Lawrence Dick, Exploration Manager. I thank all collegues that helped in one or another way, among them, geologist Alejandro Cecioni (Chief of Project), Carlos Telléz, Dr. Jorge Injoque.

I would also like to thank Dr. Carlos Palacios, who gave me constant support on all my thesis work. Finally, I give thanks to all people who at some point gave their help in the development of work required to finish this study.

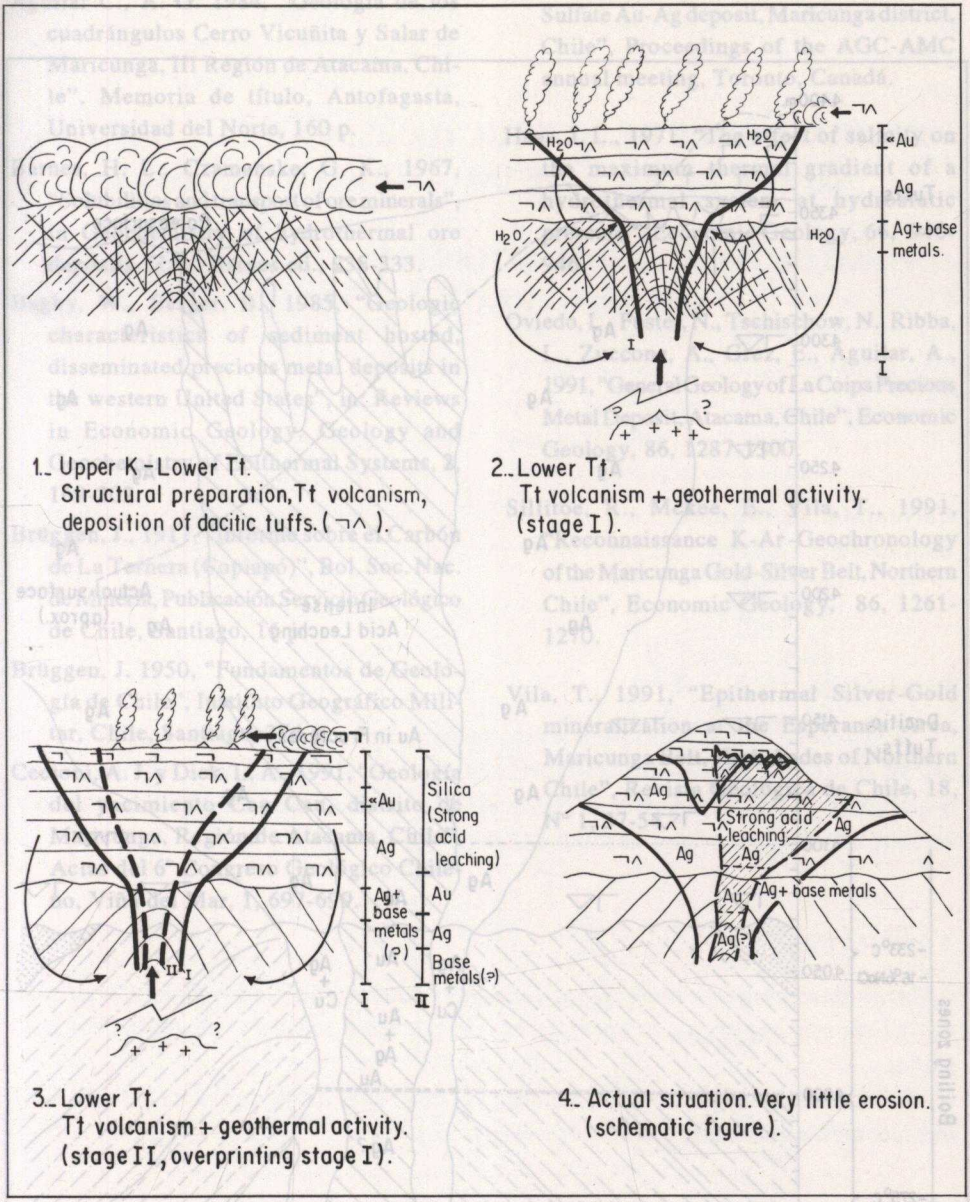

Fig. 6 Schematic evolution of Can Can.
Evolución esquemática de Can Can.

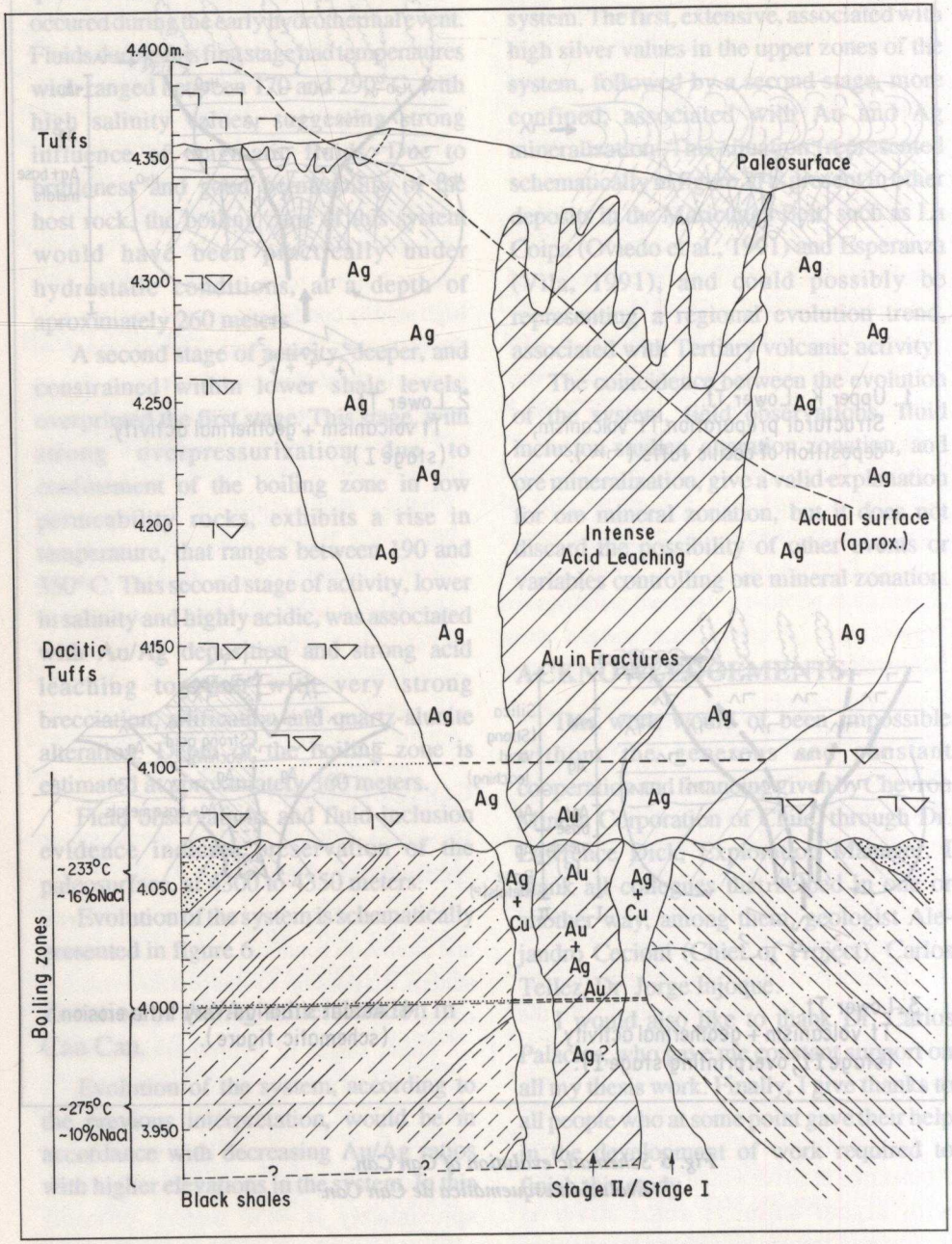

Fig. 7 Schematic reconstruction of Can Can. Au/Ag zonation.
Reconstrucción esquemática de Can Can. Zonación Au/Ag.

REFERENCES

Aguilar C., A. G. 1984, "Geología de los cuadrángulos Cerro Vicuñita y Salar de Maricunga, III Región de Atacama, Chile". Memoria de título, Antofagasta, Universidad del Norte, 160 p.

Barnes, H. L., Czamanske, G. K., 1967, "Solubilities and transport of ore minerals", in Geochemistry of hydrothermal ore deposits, H. L. Barnes ed., 238-333.

Bagby, W., Berger. B., 1985, "Geologiç characteristics of sediment hosted, disseminated precious metal deposits in the western United States", in: Reviews in Economic Geology. Geology and Geochemistry of Epithermal Systems, 2, 169-202.

Brüggen, J., 1917, "Informe sobre el Carbón de La Ternera (Copiapó)", Bol. Soc. Nac. de Minería, Publicación Servicio Geológico de Chile, Santiago, 16 p.

Brüggen, J. 1950, "Fundamentos de Geología de Chile", Instituto Geográfico Militar, Chile, Santiago, 374 p.

Cecioni, A. J. y Dick, L. A., 1991, "Geología del yacimiento Can Can, distrito de Maricunga, Región de Atacama, Chile", Actas del 6° Congreso Geológico Chileno, Viña del Mar, 1, 697-699.

Dick, L. A., Cecioni, A. J., and Tellez, C., 1990, "Can Can, An Epithermal Acid Sulfate Au-Ag deposit, Maricunga district, Chile", Proceedings of the AGC-AMC annual meeting, Toronto, Canadá.

Haas, J. L., 1971, "The effect of salinity on the maximum thermal gradient of a hydrothermal system at hydrostatic pressure", Economic Geology, 66, 940-946.

Oviedo, L., Fuster, N., Tschischow, N., Ribba, L., Zuccone, A., Grez, E., Aguilar, A., 1991, "General Geology of La Coipa Precious Metal Deposit, Atacama, Chile", Economic Geology, 86, 1287-1300.

Sillitoe, R., Mckee, E., Vila, T., 1991, "Reconnaissance K-Ar Geochronology of the Maricunga Gold-Silver Belt, Northern Chile", Economic Geology, 86, 1261-1270.

Vila, T., 1991, "Epithermal Silver-Gold mineralization at the Esperanza Area, Maricunga Belt, High Andes of Northern Chile", Revista Geológica de Chile, 18, N° 1, 37-54.